LIGHTCURVES OF THIRTEEN ASTEROIDS

Eric V. Dose
3167 San Mateo Blvd NE #329
Albuquerque, NM 87110
mp@ericdose.com

(Received: 2023 July 10)

We present lightcurves and synodic rotation periods for thirteen asteroids measured in the first half of 2023.

We present asteroid lightcurves obtained via the workflow process described by Dose (2020) and later improved (Dose, 2021). This workflow applies to each image an ensemble of typically 15-80 nearby comparison ("comp") stars selected from the ATLAS refcat2 catalog (Tonry et al., 2018). Custom diagnostic plots and the abundance of comp stars allow for rapid identification and removal of outlier, variable, and poorly measured comp stars.

The product of this custom workflow is one night's time series of absolute magnitudes, on Sloan r' (SR) catalog basis, for one target asteroid. These magnitudes are corrected for instrument transforms, sky extinction, and image-to-image ("cirrus") fluctuations and thus represent magnitudes at the top of earth's atmosphere. These magnitudes are imported directly into *MPO Canopus* software (Warner, 2021) where they are adjusted for distances and phase-angle dependence, fit by Fourier analysis including identifying and ruling out of aliases, and plotted.

Phase-angle dependence is corrected with a H-G model, using the *G* value minimizing best-fit RMS error across all nights' data; when we cannot estimate an asteroid's *G* value, usually due to a campaign's narrow range of phase angles, we apply the Minor Planet Center's default value of 0.15. No nightly zero-point adjustments (Delta Comps in *MPO Canopus*) were made to any session herein, other than by estimating *G*.

Lightcurve Results

Thirteen asteroids were observed from New Mexico Skies observatory at 2310 meters elevation in southern New Mexico. Images before May 24 were acquired and autoguided using a 0.35-meter SCT reduced to *f*/7.7 and an SBIG STXL-6303E CCD camera cooled to -35 C fitted with an Exoplanet/Blue Blocker (BB) filter (Astrodon). Images after May 24 were acquired, without autoguiding, using a 0.50-meter PlaneWave OTA and an SBIG AC4040M CMOS camera cooled to -15 C fitted with a GG495 yellow filter (Schott). A PlaneWave L-500 served as OTA mount.

The equipment was operated remotely via *ACP* software (DC-3 Dreams, version 8.3), running one-night plan files generated by python scripts (Dose, 2020). Exposure times targeted 2-5 millimagnitudes uncertainty in asteroid instrumental magnitude, subject to a minimum exposure of 150 seconds (before May 24) or 90 seconds (after May 24) to ensure suitable comp-star photometry, and to a maximum of 900 seconds (before May 24) or 480 seconds (after May 24).

FITS images were plate-solved by *PinPoint* (DC-3 Dreams) or *TheSkyX* (Software Bisque) and were calibrated using temperature-matched, median-averaged dark images and recent flat images of a flux-adjustable flat panel. Target asteroids were identified in *Astrometrica* (Herbert Raab). All photometric images were visually inspected; the author excluded images with poor tracking, excessive interference by cloud or moon, or having stars, satellite tracks, cosmic ray artifacts, or other apparent light sources within 12 arcseconds of the target asteroid's signal centroid. Images passing these screens were submitted to the workflow.

The BB and GG495 yellow filters allow for modest first-order transforms to yield magnitudes in the standard Sloan r' (SR) passband. In our hands, using these filters rather than a clear filter or no filter improves night-to-night reproducibility to a degree outweighing loss of signal-to-noise ratio from loss of flux.

Comparison stars from the ATLAS refcat2 catalog were selected only if they had a distance of at least 15 arcseconds from image boundaries and from other catalogued flux sources, no catalog VARIABLE flag, SR magnitude within [-1, +2] of the target asteroid's SR magnitude on that night (except that very faint asteroids used comp stars with magnitudes in the range 14 to 16), Sloan r'-i' color value within [0.10, 0.34], and absence of variability as seen in session plots of each comp star's instrumental magnitude vs time.

In this work, "period" refers to an asteroid's synodic rotation period, "SR" denotes the Sloan r' passband, and "mmag" denotes millimagnitudes (0.001 magnitude). The *G* value given in the lightcurve plot is that which optimized the Fourier fit.

716 Berkeley. Nine nights of observations of this outer main-belt asteroid support a synodic rotation period of 15.588 ± 0.001 h, agreeing with two previous reports of 15.55 h (Garlitz, 2011web) and 15.46 h (Polakis, 2021) but differing from two others: > 17 h (Lagerkvist, 1978) and 34.3 h (Behrend, 2018web). The RMS error of our Fourier fit is 11 mmag. The lightcurve is clearly bimodal and the period spectrum appears unambiguous.

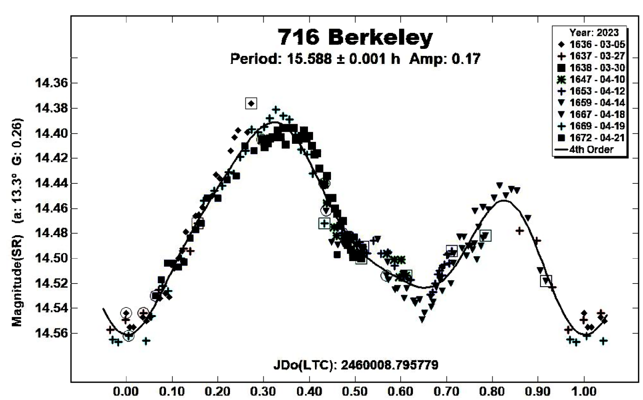

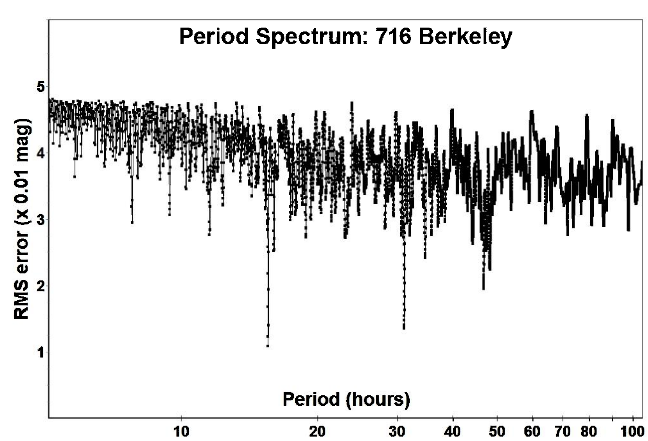

Number	Name	yyyy mm/dd	Phase	L_{PAB}	B_{PAB}	Period(h)	P.E.	Amp	A.E.	Grp
716	Berkeley	2023 03/05-04/21	*13.4,8.4	194	8	15.588	0.001	0.17	0.03	MB-O
892	Seeligeria	2023 05/05-07/06	*12.0,10.9	257	24	16.689	0.002	0.09	0.03	MB-O
907	Rhoda	2023 05/06-06/19	16.2,22.6	192	8	22.467	0.003	0.27	0.02	MB-O
920	Rogeria	2023 02/01-05/31	*7.6,23.4	145	-9	12.250	0.001	0.35	0.05	MB-M
926	Imhilde	2023 01/30-04/22	7.9,21.1	126	19	25.977	0.002	0.31	0.04	IMH
931	Whittemora	2023 04/21-06/10	*9.0,6.0	241	10	19.177	0.001	0.21	0.03	MB-O
1015	Christa	2023 04/16-05/03	11.1,6.9	240	10	11.223	0.002	0.15	0.03	MB-O
1393	Sofala	2023 02/05-04/17	*20.3,12.5	183	7	162.672	0.062	0.49	0.04	MB-I
1465	Autonoma	2023 05/29-07/05	*6.7,14.2	253	12	4.882	0.001	0.11	0.03	MB-O
1937	Locarno	2023 04/16-06/14	*9.7,20.9	221	9	110.910	0.050	0.24	0.05	MB-I
2356	Hirons	2023 04/21-06/24	*7.6,14.8	228	12	41.858	0.006	0.15	0.03	MB-O
3099	Hergenrother	2023 03/04-04/24	*9.8,17.7	177	11	25.663	0.003	0.14	0.03	MB-O
3784	Chopin	2023 04/13-07/06	*15.8,15.7	244	8	10.503	0.001	0.21	0.03	MB-O

Table I. Observing circumstances and results. The phase angle is given for the first and last date. If preceded by an asterisk, the phase angle reached an extrema during the period. L_{PAB} and B_{PAB} are the approximate phase angle bisector longitude/latitude at mid-date range (see Harris et al., 1984). Grp is the asteroid family/group (Warner 2009a).

892 Seeligeria. For this outer main-belt asteroid, we find a complex lightcurve shape yielding only one suitable period solution of 16.689 ± 0.002 h, in agreement with most previous reports: 16.7 h (Behrend, 2007web; 2017web), 16.695 h (Behrend, 2020web), 16.6924 h (Ďurech et al., 2020), and 16.693 h (Colazo et al., 2023) but differing from 15.78 h (Shipley et al., 2008) and 8.395 h (Polakis, 2020). Colazo found a lightcurve shape remarkably similar to ours, whereas the incompleteness of Shipley's phase coverage proved problematic for such a complex lightcurve shape. Polakis' result is simply half of ours, which may result from the target's smaller amplitude during that observation period. Our Fourier fit RMS error is 12 mmag.

However complex the lightcurve, the period spectrum affords only one acceptable period solution.

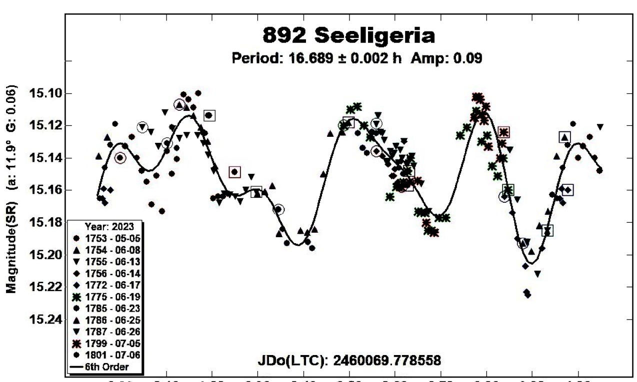

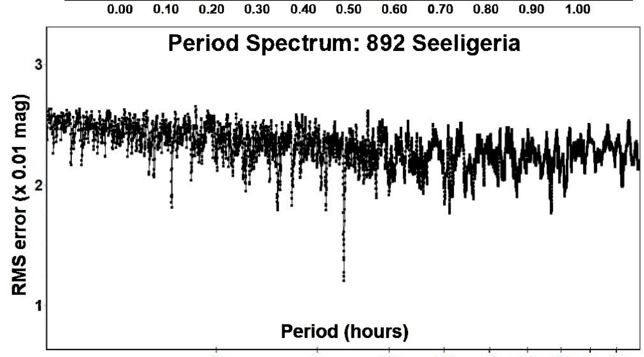

907 Rhoda. Our period estimate of 22.467 ± 0.003 h agrees well with three previous reports; 22.44 h (Warner, 2004b), 22.46 h (Marciniak et al., 2014), and 22.4 h (Behrend, 2018web); it differs from one recent survey result of 42.6307 h (Pál et al., 2020), an alias by ½ period per day. The lightcurve is clearly bimodal. Our Fourier fit RMS error is 8 mmag. The period spectrum's most significant signals are limited to multiples of our period estimate.

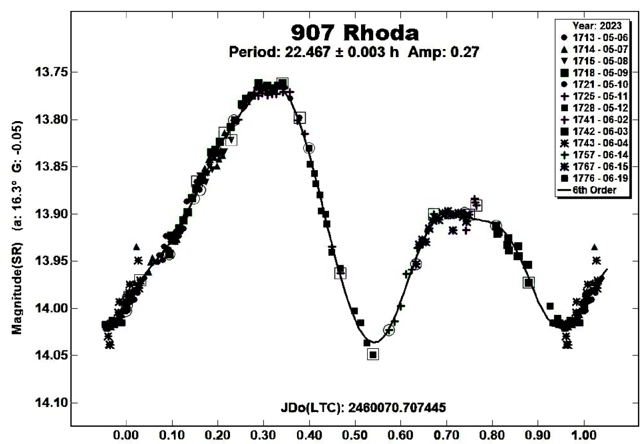

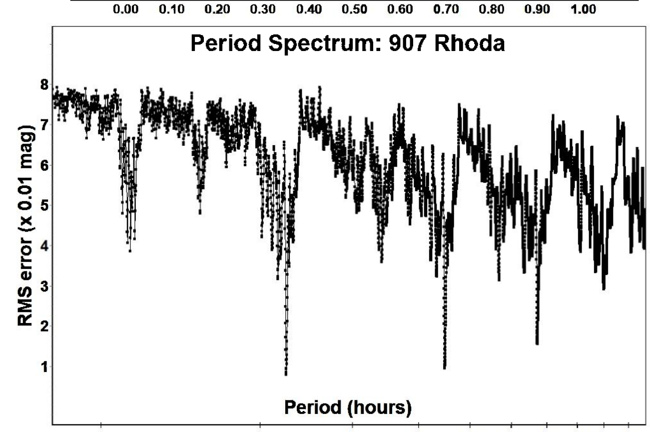

920 Rogeria. For this middle main-belt asteroid, our period estimate of 12.2500 ± 0.0005 h agrees well with two previous reports: 12.244 h (Polakis, 2018) and 12.2358 h (Pál et al., 2020), and fairly well with another of 12.5749 h (Hanuš et al., 2013) but differs from two web reports of 9.05 h (Behrend, 2012web) and 8.09 h (Pravec et al., 2012web). The 8.09 h estimate is an alias of our estimate by one period per day. Our Fourier fit RMS error is 30 mmag.

Despite 12 nights' observations over 17 weeks, our lightcurve phase coverage suffers a gap of about 20%; even so, the lightcurve is clearly bimodal. Indeed, our lightcurve observations match quite closely the shape of Polakis' 2017 lightcurve (Polakis, 2018).

Periods of 8.09 h and 9.05 h do appear as minor signals in our period spectrum, but the present period estimate dominates.

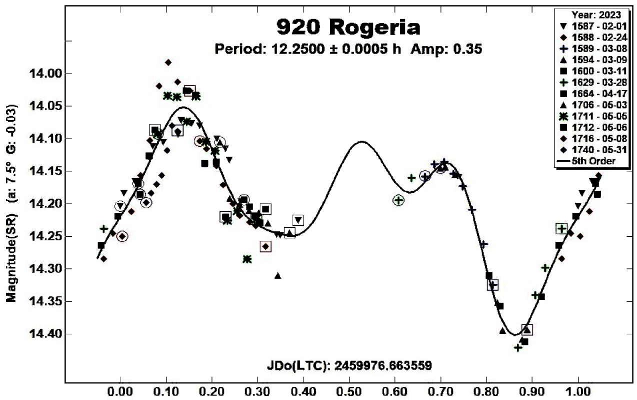

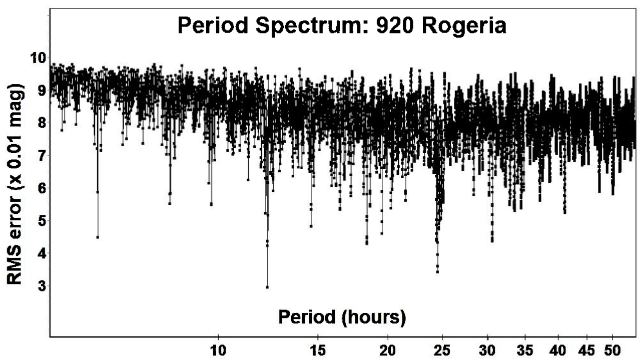

926 Imhilde. Observations of this asteroid, for which the Imhilde asteroid family is named, yield a period estimate of 25.977 ± 0.002 h, in close agreement with two previous reports: 26.1 h (Warner, 2004a) and 25.9775 h (Ďurech et al., 2020) and in rougher agreement with 26.8 h (Warner, 2011) and 25.1244 h (Pál et al., 2020). Our Fourier fit RMS error is 15 mmag.

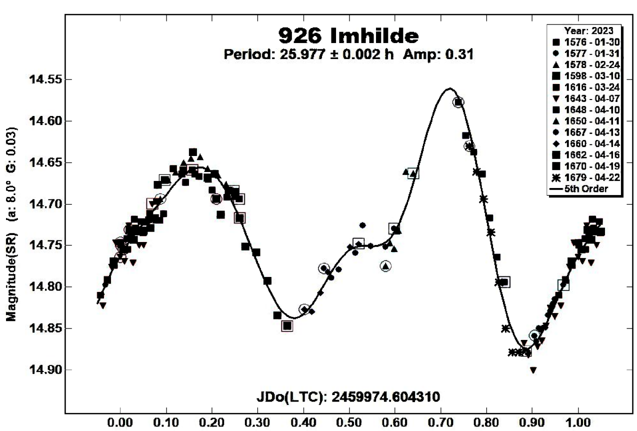

Period solutions of 26.8 h and 25.1244 h are absent from the major signals of our period spectrum.

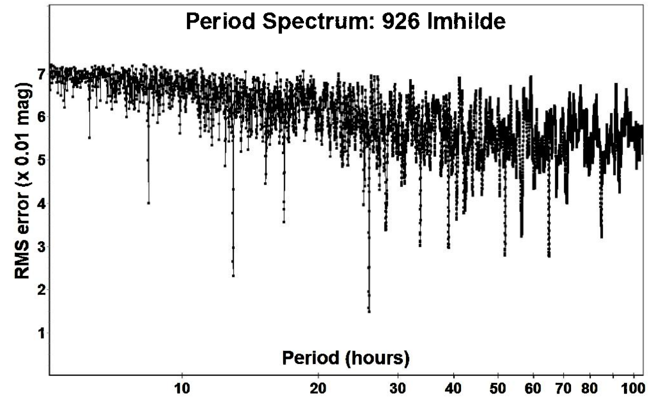

931 Whittemora. We estimate the synodic period for this outer main-belt asteroid as 19.177 ± 0.001 h, in acceptable agreement with all three known previous reports: 19.20 h (Menke, 2005), >16 h (Behrend, 2006web), and 19.199 h (Behrend, 2016web). The lightcurve shape resembles that given by Menke, except that ours shows a much sharper minimum brightness. Our Fourier fit RMS error is 10 mmag. Our proposed period and its double dominate the period spectrum.

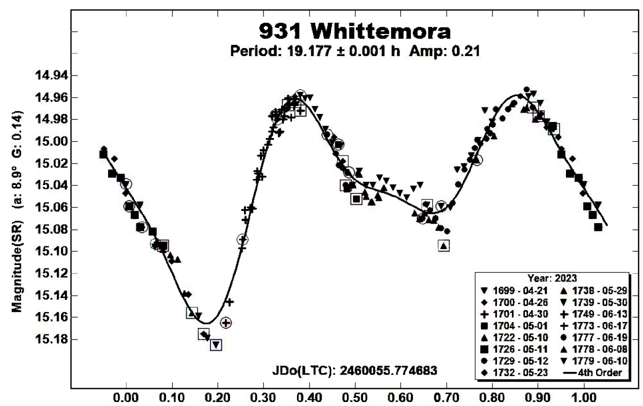

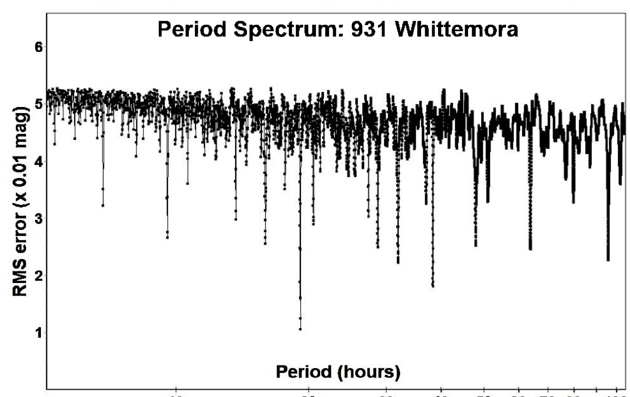

1015 Christa. We estimate for this outer main-belt asteroid a period of 11.223 ± 0.002 h, which agrees the previous reports of 11.230 h (Warner, 2009b) and 11.23 h (Colazo et al., 2020) but differs from one earlier estimate of 12.189 h (Behrend, 2005web), the latter being an alias of 11.223 h by 1 period per 6 days. Our lightcurve is roughly bimodal and resembles Warner's lightcurve shape as well as a time-reversal of Colazo's lightcurve shape. Our Fourier fit RMS error is 9 mmag.

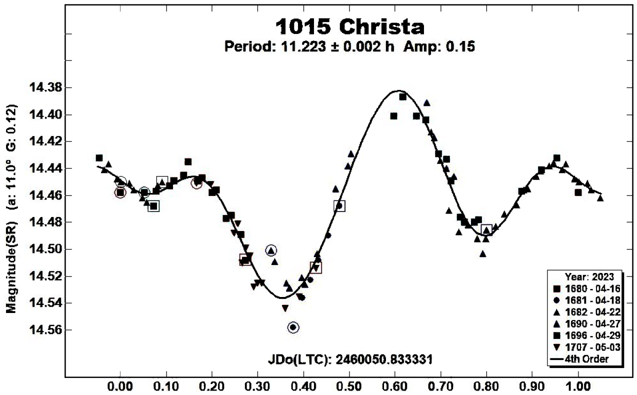

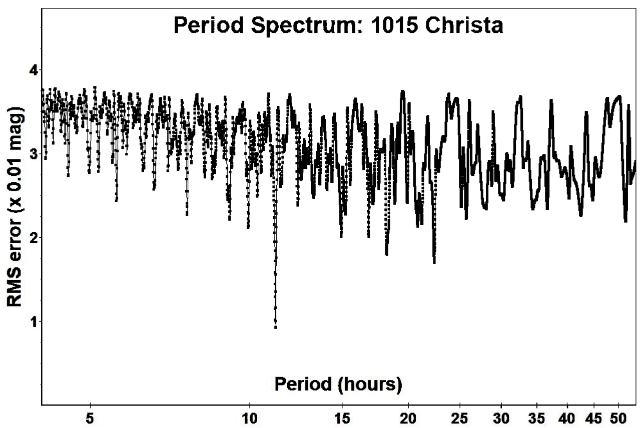

1393 Sofala. Previous reports offer three very different period estimates: 7.8 h (Behrend, 2008web), 16.5931 h (Hanuš et al., 2013), and 108.2590 h (Waszczak et al., 2015) for this inner main-belt asteroid, which is little wonder given the unusual trimodal lightcurve shape that we report here. Settling on a solution with confidence required 20 nights of observation over 10 weeks (10.5 period cycles); in the end, we report a period of 162.672 ± 0.062 h, a relatively large amplitude, and a Fourier fit RMS error of 31 mmag.

The previous estimate of 16.5931 h represents an alias of 1/3 of our estimate (monomodal interpretation) by almost exactly 1 period per day. The previous estimate of 108.2590 h is close to 2/3 of our estimate (bimodal interpretation).

The period spectrum is dominated by our period estimate, with the next three largest signals at multiples of 1/3 that estimate.

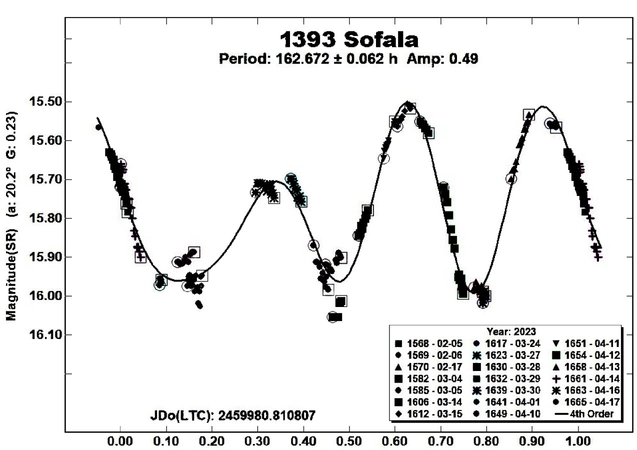

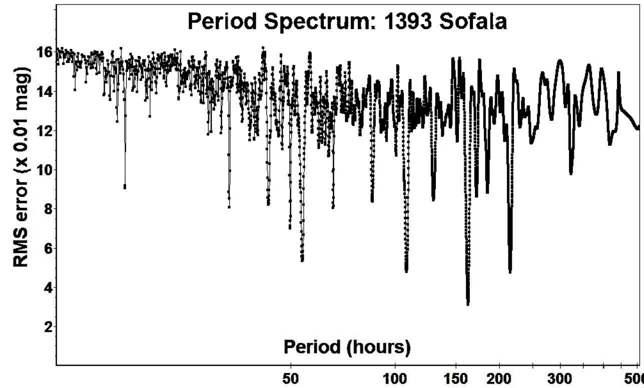

1465 Autonoma. Our period estimate of 4.882 ± 0.001 h for this outer main-belt asteroid agrees with most previous reports, e.g., 4.88 h (Brinsfield, 2008), 4.886 h (Fauvaud and Fauvaud, 2013), and 4.882 h (Ditteon et al., 2018) but differs from 11.94897 h (Ďurech et al., 2019) and 6.11 h (Yeh et al., 2020). The survey-based estimate of 6.11 h is an alias of 4.882 h by 1 period per day and its lightcurve plot shows numerous observation outliers. Our lightcurve shape is monomodal, and our Fourier fit RMS error is 11 mmag.

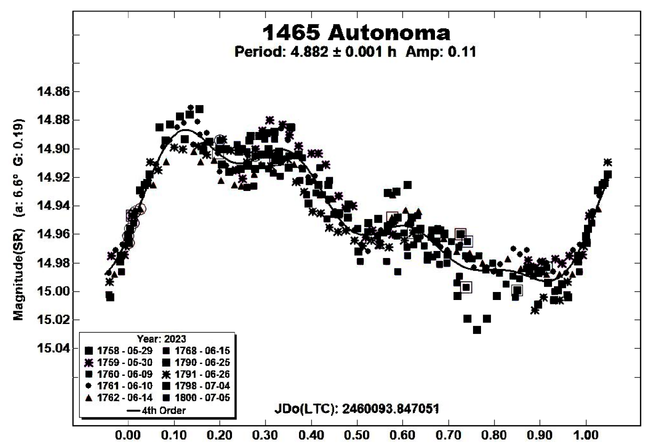

1937 Locarno. With our period estimate of 110.91 ± 0.05 h, we generally confirm the sole known previous report, 107.2 h (Behrend, 2019web) when the latter is interpreted as bimodal. Our lightcurve is bimodal as well, and the observations exhibit systematic night-to-night variations that are too large to be caused by differing sets of comp stars, possibly indicating a mild effect of precession (non-principal-axis rotation, or "tumbling"). Our Fourier fit RMS error is 21 mmag.

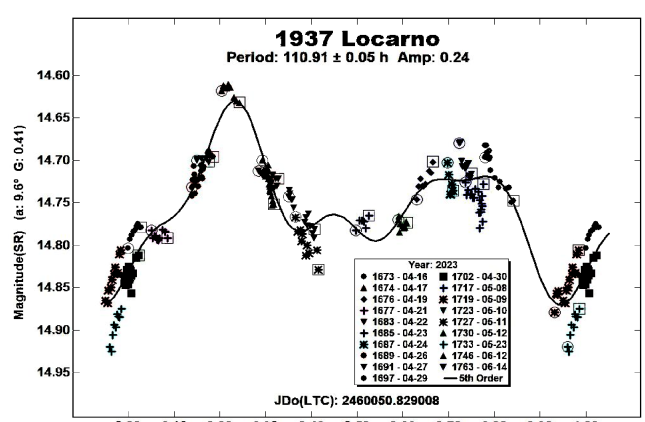

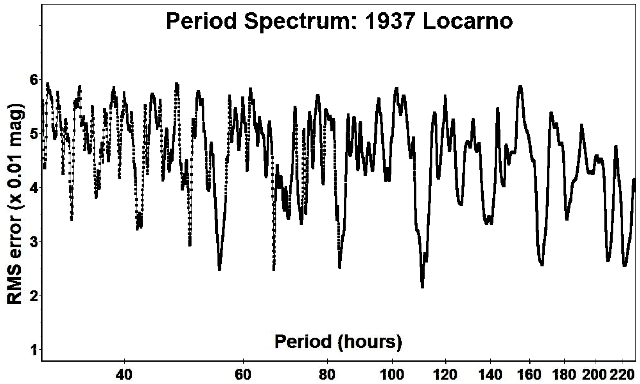

Our observations include only one night near brightness maximum, and our period spectrum shows numerous signals in addition to the main solution of 110.91 h. So, this asteroid merits re-examination with special attention to the brightness maximum and/or to the sharp brightening just prior. 2024 and 2026 apparitions favor the Northern Hemisphere.

2356 Hirons. Our period estimate of 41.858 ± 0.006 h for this outer main-belt asteroid differs from the known reports of 21.782 h (Waszczak et al., 2015) and 38.3 h (Behrend, 2020web). Our lightcurve is built from 17 nights' observations and is clearly bimodal. Our Fourier fit RMS error is 11 mmag.

We can interpret neither previously reported period as an alias, simple fraction, or multiple of our estimate, and neither appears as a major signal in our period spectrum.

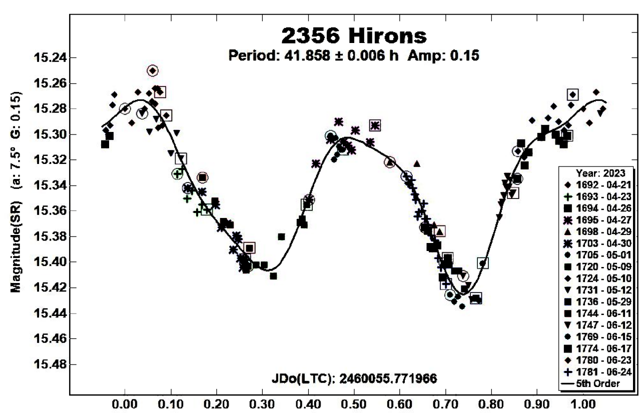

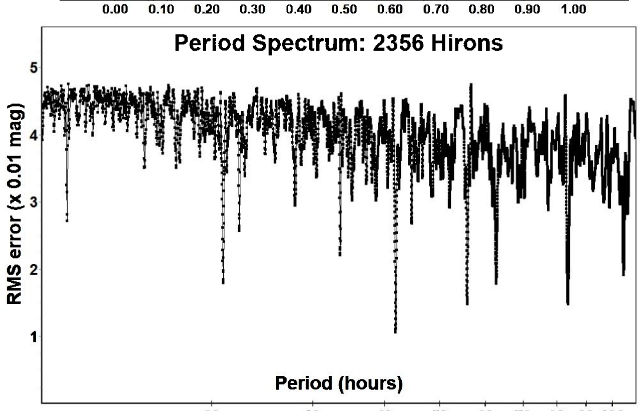

3099 Hergenrother. Our period estimate of 25.663 ± 0.003 h for this outer main-belt asteroid matches two recent reports: 25.58 h (Skiff et al., 2019) and 25.6991 h (Pál et al., 2020) more closely than it does with the 24.266 h from Behrend (2008web). Our lightcurve is bimodal and resembles the shape found by Skiff, though at only half its amplitude. Our Fourier fit RMS error is 9 mmag.

The period spectrum's major signals appear at half, one, and three-halves of our period estimate.

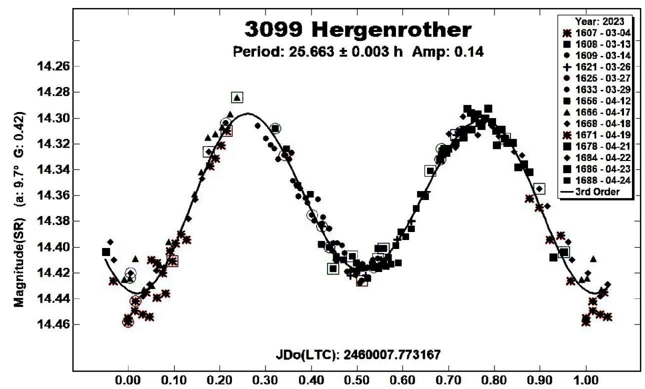

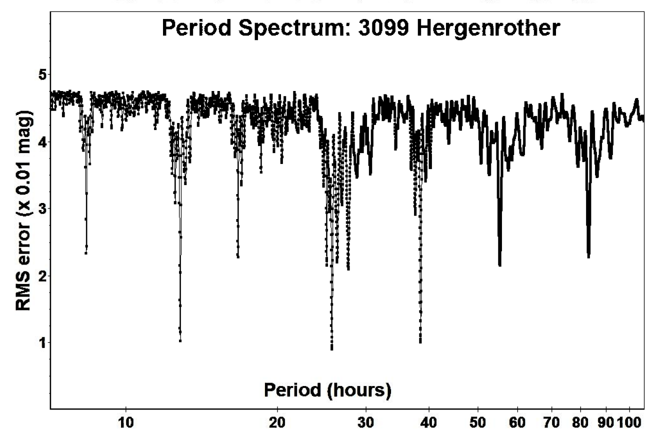

3784 Chopin. We report a rotational period of 10.503 ± 0.001 h taken as monomodal, though the amplitude and shape allow for a bimodal interpretation as well, which would agree with one previous report (20.9902 h; Pál et al., 2020) while still differing from one other (12.72 h; Behrend, 2006web). Our Fourier fit RMS error is 18 mmag.

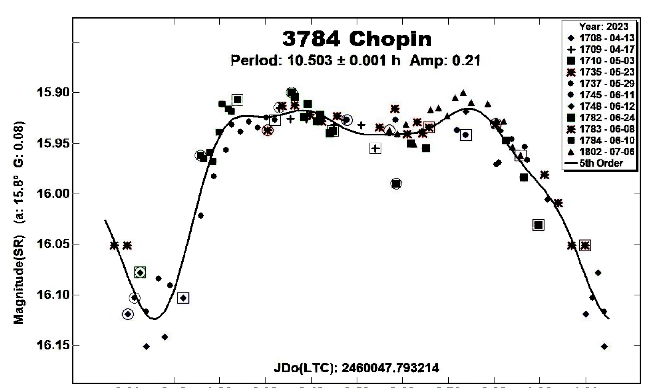

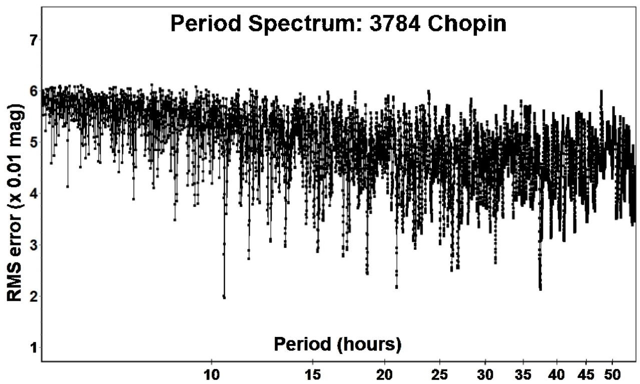

Neither the split-halves plot (not shown) nor period spectrum helps much in deciding between monomodal and bimodal interpretations. This asteroid merits observation at upcoming apparitions, which unfortunately will be fainter in magnitude than was that of 2023.

Acknowledgements

The author thanks all contributors to the ATLAS paper (Tonry et al. 2018) for providing openly and without cost the ATLAS refcat2 catalog release. This current work also makes extensive use of the python language interpreter and of several supporting packages (notably: astropy, ccdproc, ephem, matplotlib, pandas, photutils, requests, skyfield, and statsmodels), all made available openly and without cost. Thanks also to Jim Seargeant for finding and helping secure the 0.5-m OTA.

References

Behrend, R. (2005web; 2006web; 2007web; 2008web; 2012web; 2016web; 2017web; 2018web; 2019web; 2020web). Observatoire de Genève web site. *http://obswww.unige.ch/~behrend/page_cou.html*

Brinsfield, J.W. (2008). "The Rotation Periods of 1465 Autonoma, 1656 Suomi, 4483 Petofi, 4853 Marielukac, and (85275) 1994 LY." *Minor Planet Bull.* **35**, 23-24.

Colazo, M. and 20 colleagues (2020). "Asteroid Photometry and Lightcurve Analysis at Gora's Observatories." *Minor Planet Bull.* **47**, 188-191.

Colazo, M. and 16 colleagues (2023). "Asteroid Photometry and Lightcurve." *Minor Planet Bull.* **50**, 51-53.

Ditteon, R.; Adam. A.; Doyel, M.; Gibson, J.; Lee, S.; Linville, D.; Michalik, D.; Turner, R.; Washburn, K. (2018). "Lightcurve Analysis of Minor Planets Observed at the Oakley Southern Sky Observatory: 2016 October - 2017 March." *Minor Planet Bull.* **45**, 13-16.

Dose, E. (2020). "A New Photometric Workflow and Lightcurves of Fifteen Asteroids." *Minor Planet Bull.* **47**, 324-330.

Dose, E. (2021). "Lightcurves of Nineteen Asteroids." *Minor Planet Bull.* **48**, 69-76.

Ďurech, J.; Hanuš, J.; Vančo, R. (2019). "Inversion of asteroid photometry from Gaia DR2 and the Lowell Observatory photometric database." *Astron. Astrophys.* **631**, A2.

Ďurech, J.; Tonry, J.; Erasmus, N.; Denneau, L.; Heinze, A.N.; Flewelling, H.; Vančo, R. (2020). "Asteroid models reconstructed from ATLAS photometry." *Astron. Astrophys.* **643**, A59.

Fauvaud, S.; Fauvaud, M. (2013). "Photometry of Minor Planets. I. Rotation Periods from Lightcurve Analysis for Seven Main-belt Asteroids." *Minor Planet Bull.* **40**, 224-229.

Garlitz, J. (2011web). Period as given in LCDB. Web reference *http://eoni.com/~garlitzj/Period.htm* inaccessible 2023-07-08.

Hanuš, J. and 19 colleagues (2013). "Asteroids' physical models from combined dense and sparse photometry and scaling of the YORP effect by the observed obliquity distribution." *Astron. Astrophys.* **551**, A67.

Harris, A.W.; Young, J.W.; Scaltriti, F.; Zappala, V. (1984). "Lightcurves and phase relations of the asteroids 82 Alkmene and 444 Gyptis." *Icarus* **57**, 251-258.

Lagerkvist, C.-I. (1978). "Photographic photometry of 110 main-belt asteroids." *Astron. Astrophys. Suppl.* **34**, 203-205.

Marciniak, A.; Pilcher, F.; Santana-Ros, T.; Oszkiewicz; Kankiewicz, P. (2014). *ACM* **2014**, Poster 57.

Menke, J. (2005). "Asteroid lightcurve results from Menke Observatory." *Minor Planet Bull.* **32**, 85-88.

Pál, A. and 12 colleagues (2020). "Solar System Objects Observed with TESS - First Data Release: Bright Main-belt and Trojan Asteroids from the Southern Survey." *Astrophys. J. Suppl. Series* **247**, 26.

Polakis, T. (2018). "Lightcurve Analysis for Seven Main-belt Asteroids." *Minor Planet Bull.* **45**, 112-115.

Polakis, T. (2020). "Photometric Observations of Twenty-three Minor Planets." *Minor Planet Bull.* **47**, 94-101.

Polakis, T. (2021). "Photometric Observations of Seven Minor Planets." *Minor Planet Bull.* **48**, 23-25.

Pravec, P.; Wolf, M.; Sarounova, L. (2012web) *http://www.asu.cas.cz/~ppravec/neo.htm*

Shipley, H.; Dillard, A.; Kendall, J.; Reichert, M.; Sauppe, J.; Shaffer, N.; Kleeman, T.; Ditteon, R. (2008). "Asteroid Lightcurve Analysis at the Oakley Observatory - September 2007." *Minor Planet Bull.* **35**, 99-203.

Skiff, B.A.; McLelland, K.P.; Sanborn, J.J.; Pravec, P.; Koehn, B.W. (2019). "Lowell Observatory Near-Earth Asteroid Photometric Survey (NEAPS): Paper 3." *Minor Planet Bull.* **46**, 238-265.

Tonry, J.L.; Denneau, L.; Flewelling, H.; Heinze, A.N.; Onken, C.A.; Smartt, S.J.; Stalder, B.; Weiland, H.J.; Wolf, C. (2018). "The ATLAS All-Sky Stellar Reference Catalog." *Astrophys. J.* **867**, A105.

Warner, B.D. (2004a). "Rotation rates for asteroids 875, 926, 1679, 1796, 3915, 4209, and 34817." *Minor Planet Bull.* **31**, 19-22.

Warner, B.D. (2004b). "Lightcurve analysis for numbered asteroids 863, 903, 907, 928, 977, 1386 2841, and 75747." *Minor Planet Bull.* **31**, 85-88.

Warner, B.D.; Harris, A.W.; Pravec, P. (2009a). "The asteroid lightcurve database." *Icarus* **202**, 134-146. *https://minplanobs.org/MPInfo/php/lcdb.php*

Warner, B.D. (2009b). "Asteroid Lightcurve Analysis at the Palmer Divide Observatory: 2008 December - 2009 March." *Minor Planet Bull*. **36**, 109-116.

Warner, B.D. (2011). "Upon Further Review: VI. An Examination of Previous Lightcurve Analysis from the Palmer Divide Observatory." *Minor Planet Bull*. **38**, 96-101.

Warner, B.D. (2021). *MPO Canopus* Software, version10.8.4.11. BDW Publishing. *http://www.bdwpublishing.com*

Waszczak, A. and 12 colleagues (2015). "Asteroid Light Curves from the Palomar Transient Factory Survey: Rotation Periods and Phase Functions from Sparse Photometry." *Astron. J.* **150**, 75.

Yeh, T.-S.; Li, B.; Chang, C.-K.; Zhao, H.-B.; Ji, J.-H.; Lin, Z.-Y.; Ip, W.-H. (2020). "The Asteroid Rotation Period Survey Using the China Near-Earth Object Survey Telescope (CNEOST)" *Astron. J.* **160**, 73.

ROTATION PERIOD AND LIGHTCURVE DETERMINATION FOR FOURTEEN MINOR PLANETS

Mike Wiles
NAC Observatory (MPC U98)
4126 N. Twilight Cir.
Mesa, AZ 85207
mikewilesaz@gmail.com

(Received: 2023 June 28)

Photometric measurements of fourteen main-belt asteroids were conducted from 2023 February through 2023 May. Phased lightcurves and rotation periods for each one are presented here. Eight of the asteroids have no prior published period solutions. All lightcurve data has been submitted to the ALCDEF database.

CMOS and CCD observations of fourteen main-belt asteroids were performed at NAC Observatory (MPC U98) in Benson, AZ. Images were taken using a 0.35m f/7.2 Corrected Dall-Kirkham telescope. Some images were captured using a Moravian C5A-100M CMOS camera featuring a Sony IMX-461 sensor. Images were captured at a scale of 1.21 arc seconds per pixel after binning 4×4. In 2023 March the CMOS camera was decommissioned in favor of a SBIG CCD47-10 CCD camera. It utilizes a back-illuminated Teledyne E2V CCD47-10 AIMO sensor and is operated at 1×1 binning with a scale of 1.05 arc seconds per pixel. Table I shows observing circumstances and results. All images for these observations were obtained between 2023 February and 2023 May.

Data reduction and period analysis were done using *Tycho* (Parrott, 2023). The CMOS sensor provided a 58'×44' field of view, enabling the use of the same field center for three to four consecutive nights. The CCD camera provides an 18'×18' field of view. The asteroid and five or more comparison stars were measured. Comparison stars were selected with colors within the range of $0.5 < B-V < 0.95$ to correspond with color ranges of asteroids.

Comparison star magnitudes were obtained from the ATLAS catalog (Tonry et al., 2018), which is incorporated directly into Tycho. The ATLAS catalog derives Sloan *griz* magnitudes using a number of available catalogs. The consistency of the ATLAS comp star magnitudes and color indices allowed the separate nightly runs to be linked often with no zero-point offset required. The measuring aperture diameter was set to value equal to the average FWHM of the session data set multiplied by four. The same size aperture was used for asteroids and comp stars. Interference from field stars resulted in the exclusion of affected observations. Period determination was done using Tycho.

Asteroids were selected from the CALL website (Warner, 2011a), either for having uncertain periods or no reported period at all. In this set of observations, eight of the fourteen asteroids had no previous period analysis listed. The Asteroid Lightcurve Database (LCDB; Warner et al., 2009) was consulted to locate previously published results. All new data for these asteroids has been submitted to the ALCDEF database.